

# Surfactant-promoted formation of fractal and dendritic nanostructures of gold and silver at the organic–aqueous interface

Ved Varun Agrawal, G.U. Kulkarni, C.N.R. Rao \*

*Chemistry and Physics of Material Unit and DST Unit on Nanoscience, Jawaharlal Nehru Centre for Advanced Scientific Research, Jakkur P.O., Bangalore 5600064, India*

Received 19 July 2007; accepted 9 October 2007

Available online 16 October 2007

## Abstract

The effect of surfactants such as tetraoctylammoniumbromide (TOAB) and cetyltrimethylammoniumbromide (CTAB) on the type of nanostructures formed when gold ions present in the organic phase are reduced at the interface by hydrazine in the aqueous phase has been investigated. Extended fractal structures are formed at the liquid–liquid interface, the fractal structures themselves comprising cauliflower type units formed by gold nanorods. Accordingly, the nanostructures exhibit transverse and longitudinal plasmon adsorption bands in the 550 and 800 nm regions, respectively. Dendritic structures of silver are formed at the interface when Ag ions are reduced similarly in the presence of surfactants. The nanostructures consist of nanoparticles or nanorods with five-fold symmetry.

© 2007 Elsevier Inc. All rights reserved.

**Keywords:** Liquid–liquid; Fractal; Dendrites; Alloy; Nanostructures; Five-fold; Interface

## 1. Introduction

There has been a large influx of research on the synthesis and characterization of nanocrystals and related materials in the last few years [1–4]. Besides synthesis, control of the shape of nanoparticles has also received considerable attention [3,4]. Another aspect of vital interest is the assembly or self-organization of nanoparticles into different types of networks and other forms of aggregates. Thus, a few workers have been interested in the formation of fractal and dendritic nanostructures formed by metal nanoparticles [5–7]. The formation of fractals and dendrites is generally described in terms of the diffusion limited aggregates (DLA) model [8], or the cluster–cluster aggregation model [9]. Dendrites seems to be generally formed in the presence of a polymer such as polyvinylpyrrolidone (PVP) or in the presence of a template. In the present study, we have explored the formation of fractal and dendritic nanostructures of gold and silver at the liquid–liquid interface. Recent studies have shown that nanocrystalline films of

metals are formed at the liquid–liquid interface, when metal precursors in the organic phase react with reducing agents in the aqueous phase [10–12]. We have investigated the effect of a surfactant such as tetraoctylammoniumbromide (TOAB) and cetyltrimethylammoniumbromide (CTAB) present in the organic and aqueous phase respectively, on the formation of nanostructures of Au and Ag at the liquid–liquid interface. In addition, we have examined the effect of adding PVP on the nanostructure formed at the interface. The study has revealed that the surfactants do indeed favor the formation of fractal and dendritic nanostructures at the interface.

## 2. Experimental

We have employed two methods to investigate the effect of surfactants on the nature of the Au and Ag nanostructures formed at the liquid–liquid interface. In method 1, the first step involved the phase transfer of  $\text{AuCl}_4^-$  (16  $\mu\text{mol}$ ) or  $\text{AgNO}_3$  (16  $\mu\text{mol}$ ) into the organic phase (toluene, 10 ml) by TOAB (3.6  $\mu\text{mol}$ ), followed by the addition of triphenylphosphine ( $\text{PPh}_3$ , 16  $\mu\text{mol}$ ). The addition of  $\text{PPh}_3$  changes the color of the organic layer from deep orange to colorless. In the second step,

\* Corresponding author.

E-mail address: [cnr Rao@jncasr.ac.in](mailto:cnr Rao@jncasr.ac.in) (C.N.R. Rao).

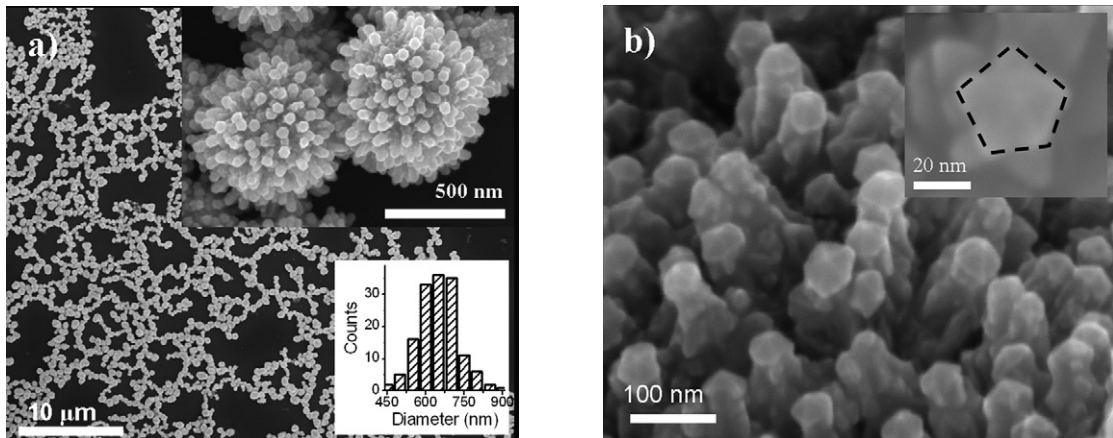


Fig. 1. (a) SEM image showing the fractal network formed by cauliflower-like gold structures by employing method 1 with TOAB. The inset on the top right corner shows a high-resolution image of the cauliflower-like structures. The inset at the bottom shows the histogram of the size distribution of cauliflower-like structures. (b) High resolution SEM image of the nanorods present in the cauliflower-like structures. Inset shows the end of one such nanorod, with a five-fold symmetry.

hydrazine (50  $\mu$ l, 0.5 mmol) was gently added to the aqueous layer (16 ml) to initiate the reduction at the interface. To obtain dendritic structures of Ag, the concentration of  $\text{AgNO}_3$  was increased (48  $\mu$ mol). In method 2, an organometallic precursor such as  $\text{Au}(\text{PPh}_3)\text{Cl}$  or  $\text{Ag}(\text{PPh}_3)_4\text{NO}_3$  was taken along with TOAB in the toluene phase. In a typical preparation, 16  $\mu$ mol of the metal precursor in toluene (10 ml) formed the top organic layer. Hydrazine (0.5 mmol) was then added to the aqueous phase (16 ml) to carry out the reduction. We have also carried out experiments following method 2 by using an aqueous solution of CTAB (5.5  $\mu$ mol in 16 ml) instead of TOAB in the organic phase. The concentration of the surfactants used by us is below the critical micellar concentration. In the case of silver nanostructures some amount of  $\text{AgBr}$  during the phase transfer of Ag ions from water to toluene formed gets precipitated (first step, method 1), this was washed off before proceeding to step 2 for reduction.

We have carried out experiments in the presence of PVP in the organic phase using method 2. The procedure was as follows. 2 mg of PVP (MW 40,000) was dissolved in 0.5 ml chloroform and the solution was mixed with 10 ml of toluene containing 16  $\mu$ mol of  $\text{Au}(\text{PPh}_3)\text{Cl}$ . The whole mixture was ultrasonicated for 2 min. The aqueous phase contained 50  $\mu$ l of hydrazine in 16 ml of water.

Transmission electron microscope (TEM) images were recorded using a JEOL 3010 operating at 300 kV. A copper grid coated with thin carbon film was carefully dipped in to the liquid system vertically so as to reach the interface piercing the film. A tiny portion of the film was lifted by the grid, which was left to dry overnight. Similarly, films deposited on silicon wafers were used for scanning electron microscopy (SEM) and energy dispersive X-ray analysis (EDAX) measurements on a FEI Nova 600 microscope. X-ray diffraction (XRD) measurements on the films deposited on glass were made with a Seifert 3000 TT diffractometer ( $\text{CuK}\alpha$  radiation). These measurements show that the films at the interface consisted of Au or Ag metal particles. UV-visible absorption spectra was recorded with a Perkin-Elmer Lambda 900 spectrometer.

### 3. Results and discussion

Fig. 1a shows a SEM image of the structure obtained at the liquid–liquid interface from the reduction of gold ions by hydrazine employing method 1. At the micron scale, the structure has a fractal type network. We estimate the fractal dimension (Hausdorff dimension) of the structure to be  $\sim 1.7$  [13]. On careful examination at higher-resolution, we find that the fractal structures are found to comprise cauliflower-like spherical units (see top inset of Fig. 1a) with a diameter of  $\sim 700$  nm (see lower inset in Fig. 1a). Pentagonal nanorods project out of the spherical units (Fig. 1b), the average density of such nanorods on the surface being typically  $\sim 200$  rods per  $\mu\text{m}^2$ . The average radius of the pentagonal face of the nanorods is 23 nm, the height being 110 nm (Fig. 2a). The inset in Fig. 2a shows a high-resolution TEM image of one such nanorod. What we actually obtain are sheets containing networks of cauliflower-like structures with the nanorods emerging from them. In Fig. 2b, we show a high-resolution image of the tip of a nanorod in its early stage of growth. The five twin boundaries are clearly discernible. We also obtain similar fractal structures comprising cauliflower-like structure when method 2 involving the reduction of  $\text{Au}(\text{PPh}_3)\text{Cl}$  with hydrazine followed by the addition of TOAB, was employed. Since we obtain similar structures by both methods 1 and 2, we conclude the role of the TOAB surfactant in the organic phase to be crucial.

Fig. 3a shows the structures formed at the liquid–liquid interface using method 1 in the absence of  $\text{PPh}_3$ . In this case, the organic layer had only  $\text{AuCl}_4^-$  ions and TOAB. Yet, we obtain fractal-like structures with a fractal dimension of  $\sim 1.8$ . These structures are highly reproducible and well connected (see inset in Fig. 3a) and are actually formed by octahedral Au crystals of the type described by Li et al. [14] (see bottom inset in Fig. 3a). Li et al., however, obtained such crystals by a modified polyol process in a PEG600 solution. The fractal structures grow denser over longer periods of time, as shown in Fig. 3b.

XRD patterns of the films at the interface confirmed the presence of metallic gold. In Fig. 4, we show the optical absorption spectra of the films which reveal broad features due to plas-

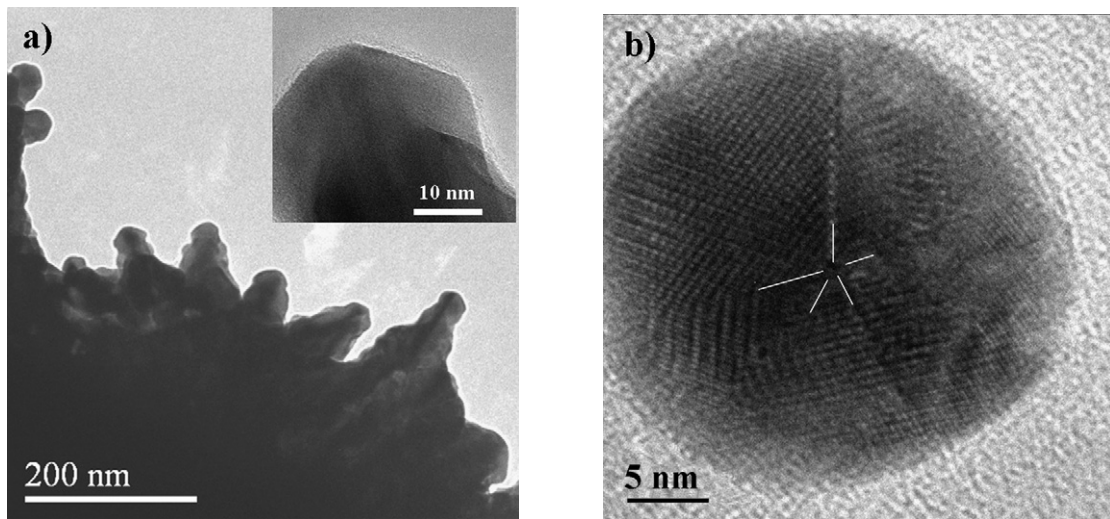


Fig. 2. (a) TEM image of a cauliflower-like structure showing tips of the nanorods. The inset shows a high-resolution image from one such rod. (b) High-resolution TEM image of a nanorod in its early stage of growth (formed after 5 min using method 1).

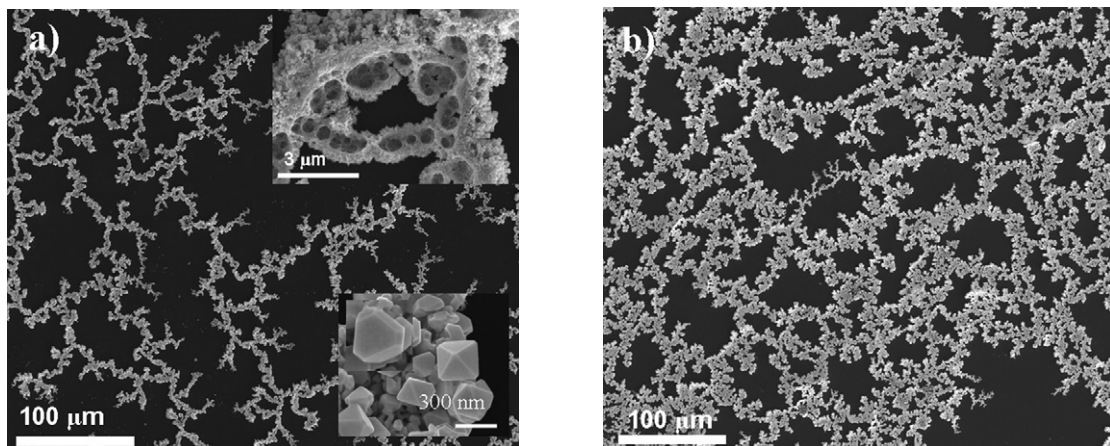


Fig. 3. (a) SEM image of the network of Au nanostructures obtained by method 1 using TOAB in the absence of  $\text{PPh}_3$  after 2 h of reaction time. The top inset shows a high-resolution image and the bottom inset shows octahedral crystals forming these structures. (b) SEM image of the network obtained after 48 h.

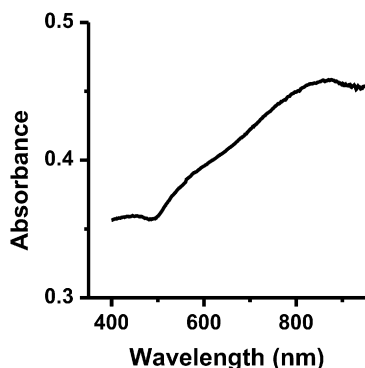


Fig. 4. Optical absorption spectrum of the cauliflower-like units comprising Au nanorods showing plasmon absorption bands.

mon absorption. The long wavelength feature around 860 nm is clearly due to aggregates of the Au nanoparticles. Such bands are characteristic of nanorods [15,16]. Electrical transport measurements showed metal-like conductivity, revealing that the structures are electrically connected. Conduction in such a random structure would be due to percolation [17].

The nanorods emanating from the cauliflower structures (Fig. 1) owe their presence to the surfactant TOAB, which is known to induce the cylindrical shapes in gold nanostructures [18,19]. The concentration of TOAB affects the number of nanorods projecting from the cauliflower-like structures. When the concentration was increased to 5 and 25 times, the density of nanorods dropped from 200 per  $\mu\text{m}^2$  to around 70 and 25, respectively. In Fig. 5, we show the kind of structures we obtained with high concentrations of TOAB (18 and 91  $\mu\text{mol}$ ). On increasing the surfactant concentration, the surface of the cauliflower-like structures become smoother and less structured. It is noteworthy that unlike the organization of large structures at the air–water interface reported by Jin et al. [20], we obtain cauliflower-like structures at the liquid–liquid interface, which further organize themselves in the form of fractals at the interface. Such an assembly is likely to be due to diffusion-limited aggregation [8]. The interface being two-dimensional (between two liquids), the formation of such structures can be described schematically as in Fig. 6. It is noteworthy that the nanorods terminate with an icosahedral face (see Fig. 1). Though not

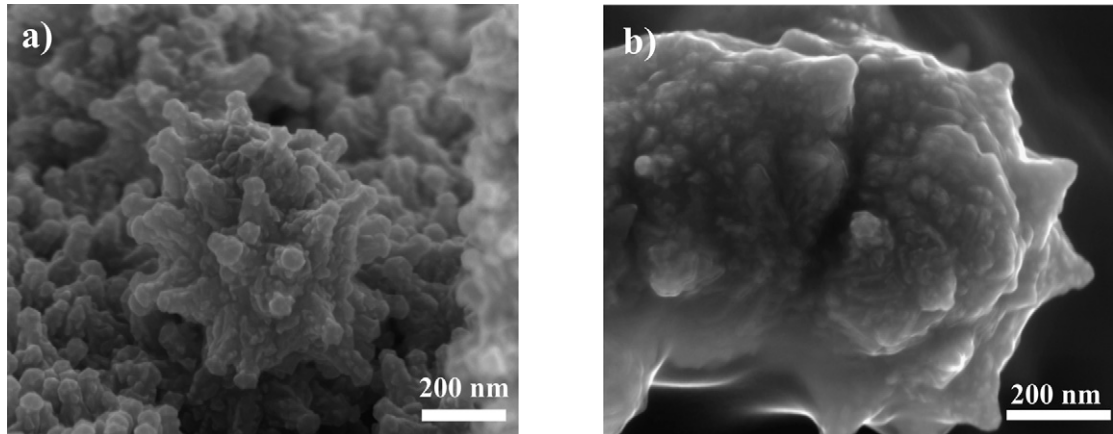


Fig. 5. SEM images of the Au nanostructures obtained by method 1 using different concentrations of TOAB: (a) 18  $\mu$ mol and (b) 91  $\mu$ mol. Other conditions remain similar as in Fig. 1.

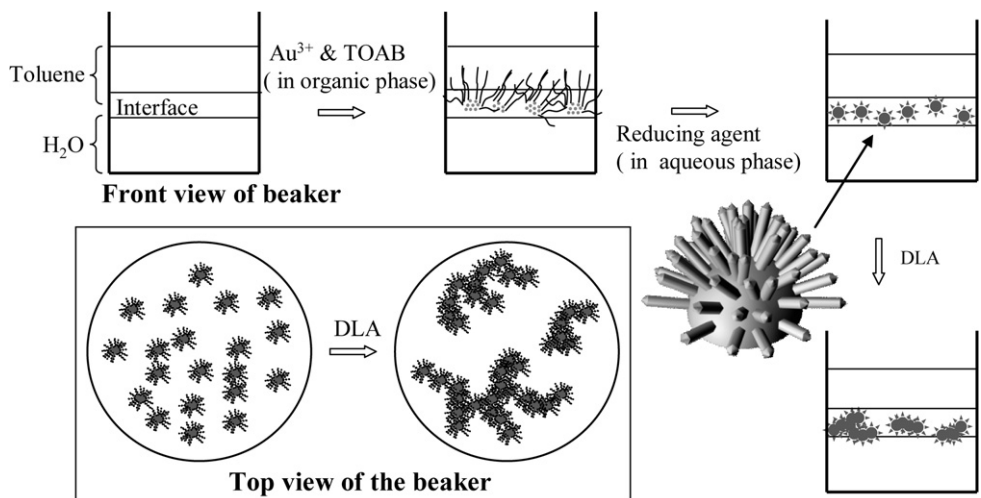


Fig. 6. Schematic showing the formation of fractal network structures at the interface.

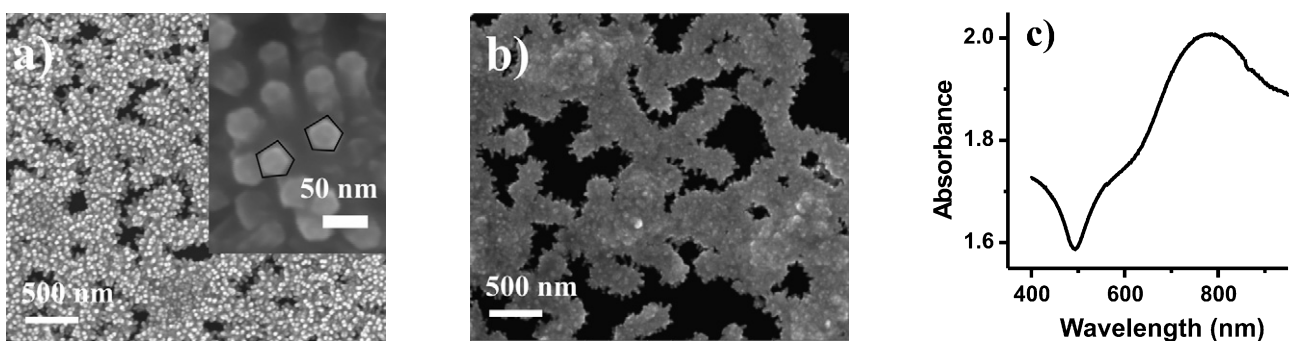


Fig. 7. (a) SEM image showing a compact network of cauliflower-like structures by method 2 using CTAB. Inset shows a high-resolution SEM image of the end (tip) of nanorods with a five-fold symmetry. (b) Image of network facing the aqueous layer. (c) Optical absorption spectrum of the network shows plasmon absorption band.

common, there are reports of the formation of five-fold structures in the literature [21,22]. Multiple twinning in gold often occurs in particles larger than 8 nm by coalescence of primary particles with tetrahedral morphology [23]. Molecular dynamics studies on the growth of small Ag nanocrystals show that icosahedral structures are energetically more favorable [24,25]. The TEM image of a Au nanoparticle (formed after 5 min of

the reaction) shown in Fig. 2b indicates the presence of multiple twin boundaries in five-fold symmetry. The five-fold rotational symmetry probably occurs due to the formation of an early twin boundary in the freshly reduced Au crystals [26].

Experiments carried out with CTAB in the aqueous phase (by following method 1) also gave cauliflower-like structures (diameter 400 nm) at the interface. In Fig. 7a, we show a

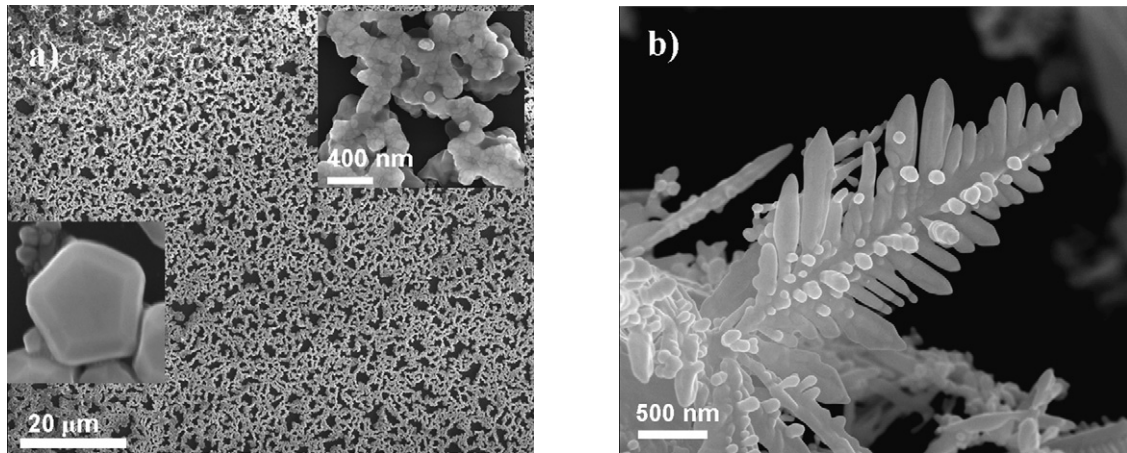


Fig. 8. (a) SEM image of the silver network obtained by method 1. The top inset shows a magnified image of the network. The bottom inset shows an icosahedral crystal. (b) Dendritic nanostructure of Ag.

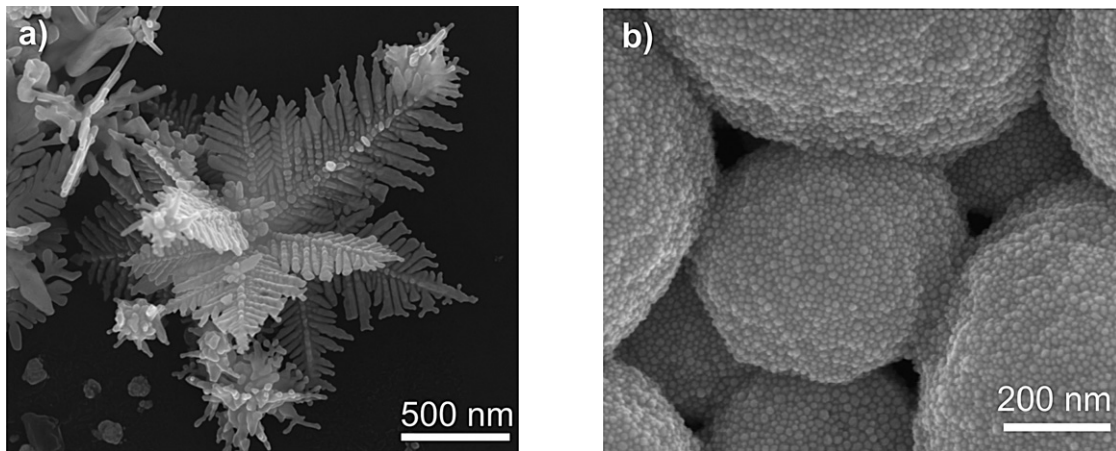


Fig. 9. SEM images of Au:Ag alloy nanostructures obtained by method 1: (a) 15:85, (b) 75:25.

SEM image of an assembly of cauliflower structures obtained with CTAB. These are densely packed in comparison to those from TOAB (Fig. 1a), but the density of nanorods on each cauliflower-like structure is similar in the two cases (see Fig. 1b and the inset in Fig. 7a). Interestingly, the growth of the nanorods is not appreciable on the aqueous side of the interface (Fig. 7b). The optical absorption spectrum of the film containing these networks show plasmon bands. The 780 nm band can be considered to be due to the plasmon adsorption of the aggregates as described in the literature [27–29].

In the case of silver, we have obtained well-connected network structures by method 1 using TOAB as the surfactant (Fig. 8a). The top inset of the figure shows an enlarged image of the network. These structures are devoid of pillars and other features observed in the case of gold. We have obtained icosahedral crystals in the reactions carried out in the absence of  $\text{PPh}_3$  (see the bottom inset of Fig. 8a). When the concentration of the Ag precursor was increased, large dendritic nanostructures were formed, as shown in Fig. 8b. Dendritic nanostructures of Ag have been produced by microwave or ultraviolet irradiation of  $\text{AgNO}_3$  in the presence of PVP [30,31]. Ag dendrites have been obtained by the interaction of tetrathiafulvalene with  $\text{AgNO}_3$  in the presence of PVP [32]. Dendrite nanostructures

are also obtained with the assistance of ultrasonic waves by using Raney nickel as the template as well as the reducing agent [33]. In all these cases, diffusion limited aggregation has been invoked to explain the formation of dendrites [34].

We have been able to obtain dendritic nanostructures of Au–Ag alloys similar to those in Fig. 8b by taking both Au and Ag ions in the organic phase. We show the results obtained with two different ratios of Au:Ag ratios (15:85 and 75:25) in Fig. 9. It is remarkable that the observed structures are drastically different, dendrites when Ag-rich, and mesoballs when Au-rich.

Experiments carried out on gold films formed at the interface in the presence of PVP (but in the absence of a surfactant) in the organic phase have also yielded interesting results. The toluene layer containing chains of Au nanoparticles of 10–20 nm diameter (Fig. 10a) turns blue. The optical absorption spectrum of the organosol shows longitudinal and transverse plasmon bands at 684 and 540 nm respectively due to the presence of the chains (Fig. 10b). The longitudinal plasmon band occurs at a relatively lower wavelength due to poorer coupling in comparison with well formed nanorods. We however failed to obtain fractal and dendritic nanostructures in the presence of PVP.

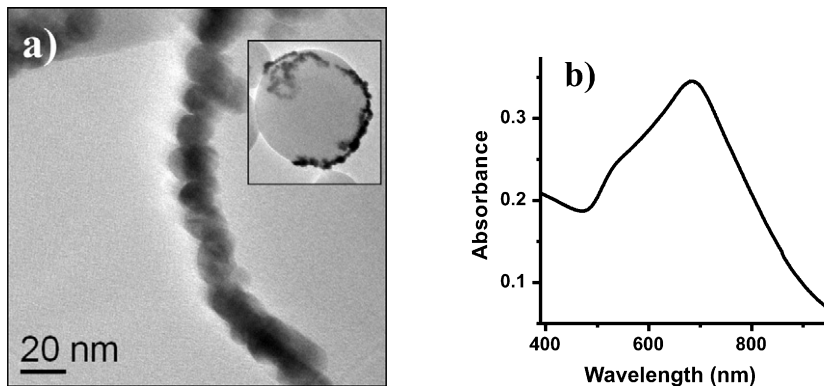


Fig. 10. (a) TEM image of a chain of gold nanoparticles decorated on PVP. Inset shows one such PVP ball decorated with a gold nanoparticle chain. (b) Optical absorption spectrum from the same, showing plasmon absorption bands.

#### 4. Conclusions

The present study shows that in the presence of a surfactant such as TOAB and CTAB, fractal and dendritic nanostructures of Au and Ag are formed at the liquid–liquid interface. This becomes possible because the surfactant molecules go to the interface and enable these structures to be formed even at low surfactant concentrations. Aggregation of the surfactant molecules appears to give rise to clusters of gold ions at the head of the surfactant molecules. After reduction, they form gold clusters and then cylindrical rods, which then aggregate to form the large cauliflower-like units. These units are involved in the formation of fractal and dendritic structures as illustrated in Fig. 6. It appears that the liquid–liquid interface provides a favorable medium for the self-assembly of nanoparticles [35]. It should be noted that the formation of fractals reported here is different from the case where preformed nanoparticles of polymers, gold and other materials are introduced into the oil or water layer [6]. We must also point out that dendrite structures of metal and semiconductor nanoparticles can be produced in the presence of electric fields during the vapor phase synthesis of nanoparticles by laser vaporization [36].

#### References

- [1] B.L. Cushing, V.L. Kolesnichenko, C.J. O'Connor, *Chem. Rev.* 104 (2004) 3893.
- [2] C.N.R. Rao, A. Müller, A.K. Cheetham, *Nanomaterials Chemistry: Recent Developments and New Directions*, Wiley–VCH, New York, 2007.
- [3] C.N.R. Rao, P.J. Thomas, G.U. Kulkarni, *Nanocrystals: Synthesis, Properties and Applications*, Springer-Verlag, Berlin, 2007.
- [4] C. Burda, X. Chen, R. Narayanan, M.A. El-Sayed, *Chem. Rev.* 105 (2005) 1025.
- [5] R. Seshadri, G.N. Subbanna, V. Vijayakrishnan, G.U. Kulkarni, G. Ananthakrishna, C.N.R. Rao, *J. Phys. Chem.* 99 (1995) 5639.
- [6] J.J. Benkoski, R.L. Jones, J.F. Douglas, A. Karim, *Langmuir* 23 (2007) 3530.
- [7] T. Reuter, O. Vidoni, V. Torma, G. Schmid, L. Nan, M. Gleiche, L. Chi, H. Fuchs, *Nano Lett.* 2 (2002) 709.
- [8] T.A. Witten, L.M. Sander, *Phys. Rev. B* 27 (1983) 5686.
- [9] P. Meakin, *Phys. Rev. Lett.* 51 (1983) 1119.
- [10] C.N.R. Rao, G.U. Kulkarni, P.J. Thomas, V.V. Agrawal, P. Saravanan, *J. Phys. Chem. B* 107 (2003) 7391.
- [11] V.V. Agrawal, P. Mahalakshmi, G.U. Kulkarni, C.N.R. Rao, *Langmuir* 22 (2006) 1846.
- [12] C.N.R. Rao, G.U. Kulkarni, V.V. Agrawal, U.K. Gautam, M. Ghosh, U. Tumkurkar, *J. Colloid Interface Sci.* 289 (2005) 305.
- [13] D.A. Weitz, M. Oliveria, *Phys. Rev. Lett.* 52 (1984) 1433.
- [14] C. Li, K.L. Shuford, Q.H. Park, W. Cai, Y. Li, E.J. Lee, S.O. Cho, *Angew. Chem. Int. Ed.* 46 (2007) 3264.
- [15] W.P. Stuart, M. Paul, *J. Appl. Phys.* 99 (2006) 123504.
- [16] J. Perez-Juste, I. Pastoriza-Santos, L.M. Liz-Marzan, P. Mulvaney, *Coord. Chem. Rev.* 249 (2005) 1870.
- [17] M.B. Isichenko, *Rev. Mod. Phys.* 64 (1992) 961.
- [18] B. Nikoobakht, Z.L. Wang, M.A. El-Sayed, *J. Phys. Chem. B* 104 (2000) 8635.
- [19] B. Nikoobakht, M.A. El-Sayed, *Langmuir* 17 (2001) 6368.
- [20] Y. Jin, S. Dong, *Angew. Chem. Int. Ed.* 41 (2002) 1040.
- [21] C.J. Johnson, E. Dujardin, S.A. Davis, C.J. Murphy, S. Mann, *J. Mater. Chem.* 12 (2002) 1765.
- [22] A. Sánchez-Iglesias, I. Pastoriza-Santos, J. Pérez-Juste, B. Rodríguez-González, F.J.G.d. Abajo, L.M. Liz-Marzán, *Adv. Mater.* 18 (2006) 2529.
- [23] K. Yagi, K. Takayanagi, K. Kobayashi, G. Honjo, *J. Cryst. Growth* 28 (1975) 117.
- [24] F. Baletto, C. Mottet, R. Ferrando, *Phys. Rev. Lett.* 84 (2000) 5544.
- [25] F. Baletto, C. Mottet, R. Ferrando, *Phys. Rev. B* 63 (2001) 155408.
- [26] M.Z. Liu, P. Guyot-Sionnest, *J. Phys. Chem. B* 109 (2005) 22192.
- [27] C.D. Grant, A.M. Schwartzberg, T.J. Norman, J.Z. Zhang, *J. Am. Chem. Soc.* 125 (2003) 549.
- [28] V.V. Agrawal, G.U. Kulkarni, C.N.R. Rao, *J. Phys. Chem. B* 109 (2005) 7300.
- [29] V. Abdelsayed, G. Glaspey, M. Nguyen, J.M. Howe, M.S. El-Shall, *Faraday Discuss.* 138 (2007) 1.
- [30] R. He, X. Qian, J. Yin, Z. Zhu, *Chem. Phys. Lett.* 369 (2003) 454.
- [31] Y. Zhou, S.H. Yu, C.Y. Wang, X.G. Li, Y.R. Zhu, Z.Y. Chen, *Adv. Mater.* 11 (1999) 850.
- [32] X. Wang, H. Itoh, K. Naka, Y. Chujo, *Langmuir* 19 (2003) 6242.
- [33] J.P. Xiao, Y. Xie, R. Tang, M. Chen, X.B. Tian, *Adv. Mater.* 13 (2001) 1887.
- [34] M. Tsuji, M. Hashimoto, Y. Nishizawa, M. Kubokawa, T. Tsuji, *Chem. Eur. J.* 11 (2005) 440.
- [35] W.H. Binder, *Angew. Chem. Int. Ed.* 44 (2005) 2.
- [36] M.S. El-Shall, V. Abdelsayed, Y.B. Pithawalla, E. Alsharaeh, S.C. Deevi, *J. Phys. Chem. B* 107 (2003) 2882.